Deanship of Graduate Studies

Al-Quds University

Measurement of liver fat concentration using dual-source dual-energy computed tomography

Mahmoud Maher Fakhoury

M.Sc. Thesis

Jerusalem-Palestine

1446/2025

Measurement of liver fat concentration using dual-source dual-energy computed tomography

Prepared By:

Mahmoud Maher Mohammad Fakhoury

B.Sc. of Medical Imaging, Al-Quds University, Palestine

Supervisor: Dr. Mohammad Hjouj

A Thesis Submitted in Partial Fulfillment of Requirements for the degree of Master of Medical Imaging Technology/ Faculty of Medicine - Al-Quds University.

1446 /2025

Al-Quds University
Deanship of Graduate Studies
Medical Imaging Technology Program

Thesis Approval

Measurement of liver fat concentration using dual-source dual-energy computed tomography

Prepared by: Mahmoud Maher Fakhoury
Registration No: 21911946

Supervisor: Mohammad Hjouj PhD

Master thesis submitted and accepted, Date: 22 / 07 / 2024
The names and signatures of the examining committee members are as the following:

1- Head of Committee	**Dr. Mohammad Hjouj**	**Signature**
2- Internal Examiner	**Dr. Hussein Al-Masri**	**Signature**
3- External Examiner	**Dr. Ahmad Abu Arrah**	**Signature**

Jerusalem/ Palestine

1446/ 2025

Dedication

I dedicate my dissertation work to my family. A special feeling of gratitude to my loving parents, Maher and Amal, whose words of encouragement and push for tenacity ring in my ears. I also dedicate this work to my beloved wife, Noor, who has been all the time there for me to support, encourage, and help. A special thanks and gratitude to my little sister, Mai, who helped me in the editing and design.
I will always appreciate all they have done.

Mahmoud Maher Fakhoury

Declaration

I certify that this thesis submitted for the degree of master, is the result of my own research, except where otherwise acknowledged, and that thesis has not been submitted for a higher degree to any other university or institution.

Signed:

Mahmoud M. Fakhoury

Date: 22/7/2023

Acknowledgment

I am truly thankful, to Allah, who gave me the power and passion to accomplish this research thesis.

Thanks are due to my supervisor, Dr. Hjouj Mohammad, whose guidance and support through this research work have meant a lot to me.

Lastly, I wish to express my gratitude to the faculty and staff of the Graduate Studies and Medical Imaging Technology Department at Al-Quds University for their support, resources, and encouragement throughout my academic journey.

Mahmoud Maher Fakhoury

Abstract

The increase in NAFLD prevalence in the Mediterranean region, which is closely associated with diet, obesity, and metabolic syndrome, justifies research about assessing liver fat accumulation and evaluating liver fat fraction using dual-source DECT. This research outlines how DECT can be used as a safe and noninvasive alternative to liver biopsy, the current method for measuring liver fat content. Liver biopsy is not only the gold standard but also an invasive procedure that is not practical for repeated monitoring.

Five portions of fresh cow liver samples were obtained, minced, and supplemented with different amounts of melted sheep fat and iodinated contrast medium (OmnipaqueTM 300) to simulate different fat concentrations. Data were acquired using a Siemens SOMATOM Force dual-source dual-energy computed tomography (DECT) scanner with Siemens Healthineers Syngo.via using mixed image analysis and the Liver Virtual Non-Contrast (VNC) application on a VB60 workstation for fat fraction quantification.

The results showed a good correlation between the actual fat added to samples and the fat fraction percentages calculated using the DECT software. For example, when we added 5g of fat (2.4% of the total sample's weight), we obtained a 3% fat fraction, and when we inserted 20g of fat (9% of the total sample's weight), we obtained a 10% fat fraction. The study confirmed a reliable quantification of liver fat content with DECT, with high specificity and accuracy. These findings indicate that DECT may serve as an important clinical tool for the early diagnosis and monitoring of NAFLD, facilitating a noninvasive and cost-effective alternative to MRI and liver biopsy. They also indicate the important role of DECT in the evaluation and follow-up of liver health, especially in regions endemic to NAFLD, where there may be an increased liver donation pool. Future studies utilizing larger sample sizes and cross-modality comparisons are needed to improve the trustworthiness and clinical relevance of these findings.

Table of Contents

List of Tables

Table of Figures

Abbreviations

C	Contrast-enhanced sample
CM	Contrast Media
CNR	Contrast-To-Noise Ratio
CT	Computed Tomography
CTA	Angiographic Computed Tomography
EAP	Early Arterial Phase
F	Fat-containing sample
HFHC	High Fat High Cholesterol diet
HU	Hounsfield Unit
kVp	Kilovoltage Peak
LAP	Late Arterial Phase
mAs	Millie Ampere Second
MDCT	Multi-Detector Computed Tomography.
MRI	Magnetic Resonance Imaging
NAFLD	Non-Alcoholic Fatty Liver Disease
NC	Non-Contrast sample
NECT	Non-Enhanced Computed Tomography
NF	No fatty content (fat-free sample)
PP	Portal Phase
ROI	Region of Interest
Sn	Tin

VNC	Virtual non-contrast
Z number	The number of protons in the nucleus

Chapter One

Introduction

1.1 Background of The Study

Fatty liver disease or hepatic steatosis is characterized by the build-up of excess fat in the liver. It has been generally classified into mainly two general types, non-alcoholic fatty liver disease (NAFLD), and alcoholic fatty liver disease (AFLD).

Non-alcoholic fatty liver disease (NAFLD) is the leading chronic liver disease globally and is closely linked with metabolic syndrome, obesity, type 2 diabetes and dyslipidemia. NASH, fibrosis, cirrhosis, and HCC constitute a spectrum of liver disease from simple steatosis (fat accumulation) to full-blown NASH, fibrosis, cirrhosis, and even HCC. Moreover, worldwide, non-alcoholic fatty liver disease (NAFLD) is estimated to affect around 25% of the population, with even greater prevalence in Western nations, as a consequence of the obesity pandemic (Younossi et al., 2016). NAFLD pathophysiology is essentially a consequence of insulin resistance and is characterized by excessive free fatty acid delivery to the liver, increased de novo lipogenesis and reduced lipid export (Friedman et al., 2018). Simple steatosis is, in general, benign, but 20-30% of them will develop into NASH (scarring/inflammation/injury) Over time, NASH can advance to fibrosis, cirrhosis, and hepatocellular carcinoma (HCC) (Diehl & Day, 2017).

Obesity (especially visceral fat), type 2 diabetes, dyslipidemia (high triglycerides, low HDL), metabolic syndrome, sedentary lifestyle, and genetic factors (e.g. PNPLA3 gene variant) are all risk factors for NAFLD. Imaging techniques like ultrasound, MRI, or transient elastography are often used in the diagnosis of fat accumulation. Liver biopsy is the gold standard for the diagnosis of NASH and fibrosis stage, and non-invasive biomarkers (e.g., FIB-4, NAFLD fibrosis score) are used to evaluate fibrosis risk (Hao et al., 2017). Given the current lack of specific pharmacotherapies, management of NAFLD is centered on lifestyle modification, including loss of weight, increased activity, and dietary alteration. Several pharmacological treatments (e.g., vitamin E and pioglitazone) have been prescribed for patients with NASH, and newer agents focused on targeting metabolic dysregulation and fibrosis (e.g., GLP-1 agonists, FXR agonists) are being studied (Diehl & Day, 2017; Hao et al.,2017).

Alcoholic Fatty Liver Disease (AFLD) occurs when the liver becomes incapable of processing the excessive amounts of alcohol in the system, causing an accumulation of fat in the liver. It can lead to alcoholic hepatitis, fibrosis, cirrhosis, and hepatocellular carcinoma (HCC). AFLD pathophysiology: Alcohol metabolism produces toxic byproducts (acetaldehyde). These metabolites lead to oxidative stress, inflammation, and fat build-up in hepatocytes (Gao & Bataller, 2011). In the early months, AFLD can be reversed with alcohol abstinence. However, continued ethanol use can progress to alcoholic hepatitis, fibrosis, and cirrhosis. Risk factors for AFLD comprise alcohol intake (heavy use defined as >14 drinks/week), genetic predispositions (i.e., polymorphisms in alcohol-metabolizing enzymes), and concurrent liver disease conditions (i.e., hepatitis C or NAFLD). Diagnosis depends on a history of alcohol use, increased liver enzymes (with AST > ALT), along imaging or biopsy to evaluate liver damage (Diehl & Day, 2017; Friedman et al., 2018; Hao et al., 2017).

Computed tomography (CT) is a medical imaging method that uses a fine beam of X-ray radiation that irradiates the patient from multiple angles around the body. The word *tomo* is a Greek word that means section or cut, and *graphy* means to produce images; hence, the name means producing sectional images of the body using a computer. The results of these angles are multiple projections of the objects within the patient's body; these projections are then reconstructed using filtered back projection, for example, to produce two-dimensional (2D) or three-dimensional (3D) images. The computer receives the acquired data and produces the final image by sorting the different objects in the image matrix according to the

differences in their attenuation factor; this allows for distinguishing between adjacent tissues. Using a special mathematical quotation, materials have a specific Hounsfield unit (HU) number. Although CT uses the same radiation waves used in routine X-ray radiography, it still overcomes the main problem of X-ray radiography; which is the superimposition of overlying tissues (Euclid Seeram, 2015; Hayre & Chau, 2022; Kauczor et al., 2019; Mamourian Alexander C., 2013; Romans Lois E., 2018).

The image in CT is composed of pixels, which are arranged in different matrix sizes, mainly 512 x 512; it can also be 256 x 256 or 1024 x 1024 depending on the machine type and/or the image quality needed for the specific procedure (Mamourian Alexander C., 2013).

Before CT, the medical field relied on various medical imaging, including routine X-rays, pneumoencephalography, and angiographic procedures. On October 1, 1971, the first clinical images of the brain were obtained for a lady who was suspected to suffer from a frontal lobe tumor. Although the procedure took a lot of time to acquire and process, the resultant images were a revolution in the history of medicine (Mamourian Alexander C., 2013).

Sir Godfrey Hounsfield was not the first to research and dig into the invention of CT as we know it today, other researchers had tried to invest in fields other than the medical one, nevertheless, Allan Cormack contributed to the birth of this revolutionary modality as well. Allan's main field of study was dosimetry, but he noticed that to calculate the precise dose to the tissues, he should know the attenuation coefficient between the source and that tissue. Since the literature then had no material on the attenuation coefficient of superimposed materials (the main drawback of routine x-rays before CT), he developed a phantom especially for this purpose from wood and aluminum with a cobalt (^{60}Co) source. With the help of one of the students to process the data using the computer, Cormack made measurements of the phantom and published his work in 1964. This work aided in the invention of CT, and thus he has been awarded the Nobel Prize alongside Sir Hounsfield. Sir Hounsfield was a scientist concerned in the field of technology and mechanics before he asked himself a question: "Could the unknown contents of a box be calculated by taking readings through the box?". This question and his first exposure to human anatomy (by a physician in 1967) were the birth of his works on exploring and studying the ability to "read" within the human body (Mamourian Alexander C., 2013).

He used mathematical equations using a computer to reconstruct the image of a 3 by 3 matrix, and then, with the help of Stephan Bates, he reconstructed an 8 by 8 image matrix. Although the application by Hounsfield for funding at the beginning of his research was rejected, later, when his works began to emerge, he was successfully funded to proceed with his works.

He discussed many aspects of CT imaging, including the scatter and beam hardening effects on the construction of the image and the effect of windowing to view specific tissues (Ambrose, 1996; Mamourian Alexander C., 2013).

Hounsfield Units (HU) in computed tomography (CT) imaging are a standard scale of measure against the radiodensity of tissues. The scale, named for Sir Godfrey Hounsfield, the inventor of the CT scanner, assigns values based on the attenuation of X-rays as they pass through different materials. For example, air is a measurement of -1000 HU, while water is 0 HU, and thick bone (greater than,000) it usually between +400 and +3000 HU. To identify issues, these values help distinguish tissues (fat, muscle and bone, for example). The HU scale is a common tool used in medical imaging and is critical for interpreting CT scans (Mahesh, 2013).

1.2 Dual Energy Computed Tomography

Dual energy CT (DECT) is a special technique used to acquire two data sets of the same object using different energy levels of the beams, depending on the mode of DE used. DECT principle is one of the oldest ideas that Hounsfield stated in his paper; if the same area of the body was scanned by two different spectrum of radiation, 100 and 140 kV, this enables to identify the atomic number of materials within the scanned area. Different materials act differently to the change in the beam energy (Fleischmann & Boas, 2011). For example, iodine (Z=53) and calcium (Z=20) can be distinguished better on a DECT compared to conventional single energy CT. Alongside conventional grey scale images, DECT provides the radiologist with additional set of images that help to quantify, characterize, highlight, and differentiate the pathology (Hounsfield, 1973; Romans Lois E., 2018).

Because CT attenuation for a specific material depends on both the material's density (electron density) and composition (effective atomic number Zeff), as well as the effective

energy, two materials with different compositions can experience a varying relative change in their attenuation between two spectra, even if their CT values are the same in one spectrum. The dual energy CT modes differ from one vendor to another but can be classified into two main categories; prospective – where the DE must be chosen prior to the scan, and retrospective – where DE data can be obtained after the patient is scanned. The prospective category includes diverse types for different companies.

The first one includes the use of two tubes and two detectors about 90 degrees from each other. A special filter made from tin (Sn) is used to ensure spectral separation between low and high energy series. This filter also plays a role in lowering the patients' dose since it removes the low energy photons that add to the skin dose. The two systems (source-detector) rotate around the body and irradiating him with different photon spectra (as biggest a gap between the two spectra as possible). This type is a trademark for Siemens Healthineers Germany company (SHS), and one of their third-generation dual source (DSCT) was used to perform this research. The second type relies on the rapid kilo voltage peak (kVp) switching from low to high spectra with constant milli ampere second (mAs). Another vendor uses the slow kVp switching rather than fast. Siemens also has another type which depends on a special physical filter consists of two materials to filter the x-ray beam before it exists the tube, tin (Sn) part to filter the low energy photons (high spectra), and gold (Au) part to filter the high energy photons (low spectra) (Kauczor et al., 2022).

More than one vendor also has the ability to produce DECT images by scanning the patient twice, once with high energy beam and once with low energy, then the image data sets are co-registered to produce one DECT. The retrospective method is adopted by one vendor; its main principle is to scan the patient with relatively high kVp and mAs, and then on the detector level, the low energy photons are absorbed by the higher layer of the, and the higher energy photons pass through to the second layer of the detector, which produces two data sets. This technique is called a dual layer or sandwich. One of the main advantages of DECT over conventional CT is that it can separate different tissue types depending on their z number, this enables to quantify different materials within the tissues (Kauczor et al., 2022).

1.3 Problem Statement

The ability to quantify materials creates a way to check for fat saturation in the liver since liver steatosis is a severe problem in our region (Middle East) and needs to be addressed sooner rather than later (Kodama et al., 2007).

Hepatic steatosis is a disease that describes the accumulation of triglycerides within the tissue of the liver. This condition may develop, depending on its severity to several serious illnesses, such as steatosis, fibrosis, cirrhosis, and hepatocellular carcinoma. Fatty liver disease is not associated with alcohol usage only, non-alcohol fatty liver disease (NAFLD) is the most common hepatic disease in the world and is related to several fatal diseases such as obesity, diabetes mellitus, and metabolic syndrome (MS). The Middle Eastern countries (especially the Arab countries) have an obesity rate that is larger than the United States of America (USA), the rate extends from 33.1% in Egypt to 42% in Kuwait vs 33% in the USA. NAFLD is related to the individual diet, studies have found that the consumption of carbohydrates in excessive amounts, saturated fats, and protein from meat and soft drinks could cause NAFLD (Ashtari, 2015; Hur et al., 2014; Mirmiran et al., 2017).

Because effective treatment and dietary adjustments can lead to improvements in the condition, it is crucial to ascertain the extent of hepatic steatosis, which refers to the amount of fat present in liver tissue. This knowledge is essential for devising an effective treatment plan and for evaluating treatment outcomes. Although histologic examination of hepatocellular fat vacuoles remains the gold standard for assessing hepatic steatosis, liver biopsy is invasive and therefore cannot be performed frequently enough to monitor treatment response adequately. Furthermore, routine histologic examination is semiquantitative, subject to observer interpretation, and graded using broad severity categories, which can lead to sampling errors. This calls for other means for fat content measurement, magnetic resonance imaging (MRI), ultrasonography (US), and CT have been used for this purpose. Conventional CT scans have a reduced ability to detect mild to moderate hepatic steatosis, and the presence of hemosiderin deposition can prevent an accurate assessment of hepatic steatosis using CT attenuation. However, DECT can be employed to assess hepatic steatosis

by quantifying the alteration in hepatic attenuation between images acquired at lower and higher energy levels using the three-material decomposition. Fat, soft tissue, and contrast media are the materials that are used for this purpose. On one hand, soft tissue HU stays stable both for low and high kV energy datasets, and fat as well will have stable values, while iodine contrast medium HU values change between low and high kV sets drastically, with almost half the value between lower and higher energy datasets. Fat has an HU value of -50, soft tissues have a value range of 40 – 60 HU, whereas iodine has different HU values; 296 HU for 80 kV and 144 HU for 140 kV, that is a ratio of (2.06) (Kauczor et al., 2022).

Three-material decomposition (3MD) in dual-energy computed tomography (DECT) is a technique used to differentiate and quantify three distinct material components within a scanned object by exploiting the energy-dependent attenuation properties of X-rays at two different energy levels. This method assumes that the scanned volume consists of a mixture of three basis materials (e.g., soft tissue, iodine, and bone) and mathematically decomposes the attenuation values to estimate the concentration of each material, enhancing tissue characterization and lesion assessment (Johnson et al., 2007). The iodine ratio, often derived from 3MD, is a metric used to assess the relative iodine content in tissues, providing crucial functional information such as perfusion and vascularity, particularly useful in oncology and cardiovascular imaging. By leveraging these techniques, DECT enables improved contrast resolution and material-specific imaging, aiding in accurate disease diagnosis and treatment planning. The material ratio can be calculated using a simple equation that enables one to identify this material; Ratio = HU (low kV) / HU (high kV) (Kauczor et al., 2022). This formula of ratio alongside the stable reference materials enables us to quantify the percentage of fat within the liver theoretically, which is the main hypothesis of this research.

1.4 Justification

Since the previous studies were conducted either on animals or, on other DECT modes, the current study will try to calculate the exact ratio of fatty content within the liver using the virtual non-contrast (VNC) images produced in combination with the DS CT scanner and the special reporting workstation.

1.5 Study Objectives

This study can be helpful in early diagnosis of (NAFLD) since this disease may develop into a more serious condition that can be lethal.

Thus, the main aim of this study is to calculate the fatty content of liver and associate an exact severity rate to, i.e., mild, moderate, and severe hepatic steatosis.

- Secondary objective:
    - To validate the use of tool (fat saturation) itself in evaluating the fat content in liver tissue.

1.6 Study Hypothesis

Hypothesis 1: The Mediterranean food diet is a major cause of NAFLD.

Hypothesis 2: NAFLD can develop into more serious diseases like cancer.

Chapter 2

Literature Review

2.1 Introduction

Su et al. were not the first to use the rabbits in their study, but they asserted that it is very important to know the hepatic steatosis grade for the liver donation process, and how much it is considered a relatively difficult process, since there is a serious shortage in in donors and a high percent of patients have died while waiting for their turn (Su et al., 2009).

Due to the high severity of the non-alcoholic fatty liver disease (NAFLD), which is considered an important marker for future cardiovascular diseases, Huo et al., had developed an automatic tool to measure the fat content in the liver segments, automatic liver attenuation ROI-based measurement (ALARM). They used their own pre-published liver segmentation tool that was based on convolutional neural network and then 4 ROIs were calculated within the liver tissue. The authors compared the manual placement of 1 cm2 ROIs on 738 CT scans, which relied on the experience of the clinical experts with the automatic placement of the ALARM tool, they found the tool to be very accurate with the manual ROI (Huo et al., 2019).

Single energy standard scan was performed on GE scanner and used 120 kVp, as the rest of the standard single energy CT scans. 39 rabbits finished the study (out of 45), the rabbits were sorted into five groups, the first group was fed a regular diet, while the other groups were fed high fat high cholesterol (HFHC) diet for 3, 6 and twelve weeks respectively. The

fifth group was considered as supplement in case a certain rabbit died in other groups to replace it. Liver attenuation (HU) values were calculated using average region of interests (ROIs) values, and the ration between hepatic and muscular attenuation levels. Other studies were performed as well, including ultrasonography (US), MRI and histological tests. The result showed that whenever there is a high level of hepatic steatosis the hepatic attenuation values decrease (Kawata et al., 1984).

Animal models allow for a more systematic approach and extreme values of the fat content to be achieved. On the other hand, the animal liver may differ, to some extent, from the human liver so that CT-values need not be exactly the same. The animal models confirm that there is a linear relationship between fat content and CT-value, non-enhanced (NECT) CT is among the best methods to quantify fat content. As Kawata et al. (1984) pointed out, there are two types of fat that can accumulate in the liver (triglycerides, cholesterol), so that the composition of fat is not exactly defined. On the other hand, two publications mainly consider the triglyceride content of the liver, and one publication (Su et al., 2009) suggests that the triglyceride content in the blood is a better predictor for fatty liver than the cholesterol content in the blood.

Although it is thus known that there is a linear relationship between the CT-value of the liver in a non-contrast CT-scan and the fat content defined on any reasonable scale, the exact coefficients are not easily determined.

For the fat-free liver mean CT-values of 61HU or 64HU are provided in literature. But systematic deviations depending e.g., on patient diameter, scanner type, spectrum and scan mode are usually not known (Kauczor et al., 2022; Kawata et al., 1984).

Different studies have studied the hepatic and liver attenuation (HU) ratio to check for hepatic steatosis within the asymptomatic patients, such as Boyce et al., with 3357 consecutive asymptomatic patients shows that there is a rather wide spread of liver CT-values in the normal population. The measured CT-value was 59+/-10HU (mean value / standard deviation). Different CT-scanners (8 & 16 slice) were used, they were scanned using a low-dose CT colonography scan, and patients with various special clinical conditions were present such as obesity, diabetes mellitus or alcohol overuse. Hepatic and splenic HU ratio was calculated, if the value of liver HU over splenic HU is ≤ 1.1 then the patient has hepatic steatosis, and as the number decreases the severity of hepatic steatosis increases. Zeb et al., also used the L/S attenuation ratio (they determined the value to be ≤ 1.0), and the scan

performed was a non-contrast cardiac scan to check for coronary calcifications, parts of the spleen and liver visible on the images and the relative HU values were obtained. The result stated that the attenuation HU were highly reproducible (Boyce et al., 2010; Zeb et al., 2012).

Kodama et al., performed a retrospective study on 88 metastatic patient who underwent liver resection after the scans. Non-contrast, early arterial (EAP) or late arterial (LAP) and portal (PP) phases were obtained using 150 cc non-ionic iodinated contrast media. The authors compared different methods of determining CT value; the first is to check the liver HU only, the second is to calculate the difference between liver and spleen HU and the third to calculate the ratio between the liver and splenic HU. The net result was that they found measurements on non-contrast CT was best for prediction of pathologic fat content in correlation with resected liver portion that was histologically tested (Ashtari, 2015; Boyce et al., 2010; Kodama et al., 2007).

Although, the usage of contrast enhanced single energy CT scans for determining the fat content has been discussed in literature, this has not been generally accepted, since contrast agent enhancement adds an additional complication. On the other hand, also the usage of Dual Energy CT for determining the fat content based on non-contrast dual energy scans so far has demonstrated little value (Kawata, 1984; Kriston et al., 2011; Mirmiran et al., 2017; Park et al., 2006; Su et al., 2009).

Two studies were conducted on patients using fast kVp switching method for DECT and used GE's dedicated software (that is somehow different from SHS).the first study was performed prospectively on 16 rabbits that had a high cholesterol and high fat diet (HFHC) for different weeks, depending on the groups the authors created; the first group was fed a standard diet for six weeks and considered a control group, the second group was fed a standard diet for four weeks and two weeks of HFHC diet, the third group was fed standard diet for two weeks and HFHC for four weeks, while as the fourth group was fed HFHC diet the whole six weeks, this method created a different level of liver fat content. The rabbits were scanned twice using CT, first scan was a standard single energy non-enhanced scan, and the second was a dual energy scan which was used to calculate the hepatic fat fraction (HFF) using multi-material decomposition (MMD), an MRI proton density fat saturation scan and a histologic assessment of liver specimens. The result of the study was that qualification of the HFF using dual energy CECT was practical and showed comparable sensitivity and specificity to single energy UECT for the detection of hepatic steatosis. The

second study included 177 patients in two groups; the first group A (n=125) had a whole-body non-contrast DECT, and group B (n=52) underwent multiphasic (NC, arterial, porto-venous) DECT including single energy non-contrast scan, the iodinated contrast medium was administered with a ratio of about 1.5 cc/Kg. They found a strong correlation between fat percentage found with DECT and HU measured in non-contrast CT (Hur et al., 2014; Xu et al., 2022).

Chapter 3

Research Design

3.1 Methodology and Research Design

This research aims to validate the fat saturation tool of the Liver Virtual Non-Contrast (Liver VNC) application, developed by Siemens Healthineers. The main principle for image analysis in dual-energy-based scans relies on tri-material decomposition.

For ethical and practical reasons, preserved human or fresh animal tissue often substitutes fresh human tissue in medical education and research. Porcine and bovine tissues are commonly used due to their availability and similarities to human tissue (Estermann et al., 2021).

For the sample scans, liver from a freshly slaughtered cow was collected, minced using a meat grinder (Figure 1), and then divided into five nearly equal portions (214 ± 9 g) (Figure 2). Due to the viscosity and texture of the liver, the weights were not identical, and each sample's fat fraction analysis was calculated relative to the individual fat concentration. Additionally, fat was collected from freshly butchered sheep and melted Figure 3 to be added to the samples before scanning.

3.2 Research Instruments

For this study, the third generation of Siemens Healthineers AG; Forchheim, Germany scanner was used for the scanning purpose; SOMATOM Force; VB20 (192 slices x 2 detectors), which applies the dual source dual energy technology capabilities, since it has a two-tube perpendicular to each other design. For the analysis of the samples, Siemens Healthineers Germany workstation, the commercially available, Syngo.via VB60 was used as it is the special system for dual energy data analysis using different algorithms, two workflows (special tools and application within the Syngo.via system) were used; MM Reading for general viewing and attenuation measurements and analysis of mixed data images (generated image series composed of the raw data of both low and high energy data sets that are equal in quality to single energy 120 kVp images), and CT Dual Energy workflow for Liver Fat Fraction (Liver VNC) application.

3.3 Research Sample and Design

A whole cow liver (which weighed about 1100 g) was collected from a local butcher, which was butchered earlier on the same day. A small piece of sheep fat was also collected from the same shop. Iodinated contrast medium OmnipaqueTM 300 mg I/ml (Figure 4) was also used which I bought from a nearby hospital. The results (of the image analyses) of all scans were then compared to the amount of fat added.

The liver was cut into smaller portions, and then ground using the meat miner, the mixture was ground twice to get to the finest mix possible so it would be as uniform as possible. The fat piece was cut into small pieces so I could melt them down in the pan, after the suitable amount of fat was collected, I prepared the contrast medium syringes.

I have sorted the minced liver tissue in 200g pieces, almost equally. For each sample (other than the reference sample) I have added the specific amount of melted fat, and/or iodinated contrast medium. After adding the required amount of each of the materials, I used a hand

blender to mix and blend the mixture for about 5 minutes each to try to achieve maximum homogeneity possible, the mixture was uniform visually. Afterward, I froze the samples in the freezer. The next day I traveled to (Wolfson Medical Center in Occupied Palestine) and scanned each of the samples in five separate scans, the average result of the scans was registered in this study, the samples were as follows;

- The reference sample weighed 205g of minced liver tissue, which was used as a reference for all the samples, both for fat and iodine content.
- Sample number (one) consisted of 202g of minced liver tissue, and 5g of melted fat mixed using the hand blender, the net weight was 207g.
- Sample number (two) consisted of 204g of minced liver tissue, 5g of melted fat, and 3cc of iodinated contrast medium was mixed using the hand blender, with a net weight of 212g.
- Sample number (three) consisted of 200g of minced liver tissue, 20g of melted fat, and 3cc of contrast medium, with a net weight of 223g.
- Sample number (four) consisted of 196g of minced liver tissue, 10g of melted fat, and 3cc of contrast medium, with a net weight of 209g.

Figure 1. Preparing the liver for processing

Figure 2. Weighing and sorting of samples

In (Figure 2), the abbreviations on the stickers stand for:

NC: non-contrast sample, pure liver tissue without fat nor iodine,

C: contrast-enhanced sample, contrast media added to the sample,

NF: fat-free sample, no fat was added to the sample,

F: sample with added fat, melted fat was added to the sample

Figure 3. Fat preparation

Figure 4. Fat added and mixed.

3.4 Data Collection and Scan Procedure

The samples were scanned in a routine dual energy scanning protocol with the following parameters: 100 kVp and Sn150 kVp, CAREDose4D modulation algorithm was used for mAs modulation, 0.6 pitch, 0.5s rotation time, 128*0.6*1.5 mm collimation. The reconstructed mixed images slice thickness 3mm with a 3mm overlap as used in standard soft tissue reconstruction, DE datasets slice thickness 1.5*1.0 mm. No scan delay was used.

Each sample was viewed separately in Syngo.via in both of Syngo.via workflows, three circles of region of interest (ROIs) were drawn with equal sizes. All the readings were registered into MS Excel sheet in tables.

Chapter 4

Results

For image analysis, two Syngo.via workflows were used (MM Reading workflow for the basic HU readings, and CT Dual Energy workflow for the advanced algorithm of Fat Saturation within Liver VNC application), and the average value will be used for discussion, and the numbers will be rounded, all the readings will be available in the tables.

4.1 Mixed Images Analysis

As mentioned in the previous chapter; two workflows were used to analyze the images of the liver samples, and the average value will be used for discussion, and the numbers will be rounded, all the readings will be available in the tables.

Within MM Reading workflow in Syngo.via workstation, using circular region of interests measuring tool (ROI), three ROIs were drawn in each sample, three main reading results from ROI, min HU, max HU and Mean (HU).

4.1.1 Reference Sample

The reference sample Figure 5 min HU was 63, whereas the max HU was 111 (Table **1**), and the mean value was 84. According to (Huo et al., 2019), the normal value in human non-contrast liver CT is 50-75 HU.

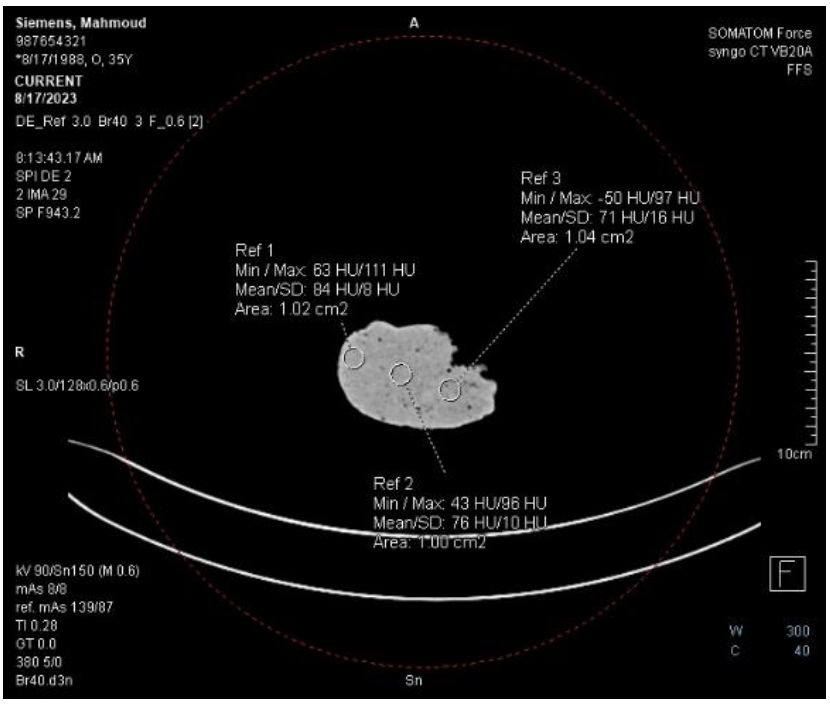

Figure 5. Reference sample analysis using MM Reading.

Table 1. Reference sample HU values

Reading	min HU	max HU	Mean	SD
1	63	111	84	8
2	43	96	76	10
3	-50	97	71	16
mean value	18.66666667	101.3333333	77	11.33333333

4.1.2 Sample Number One

Sample number one (Figure 6) had a min HU of –37, max HU of 87, and the mean was 59 HU (Table **1**). The dropdown in the HU comparing to the non-contrast is due to the injected fat, as the HU of fat ranging in the negative values on the HU scale (human fat HU average –100 HU) (Chougule et al., 2018).

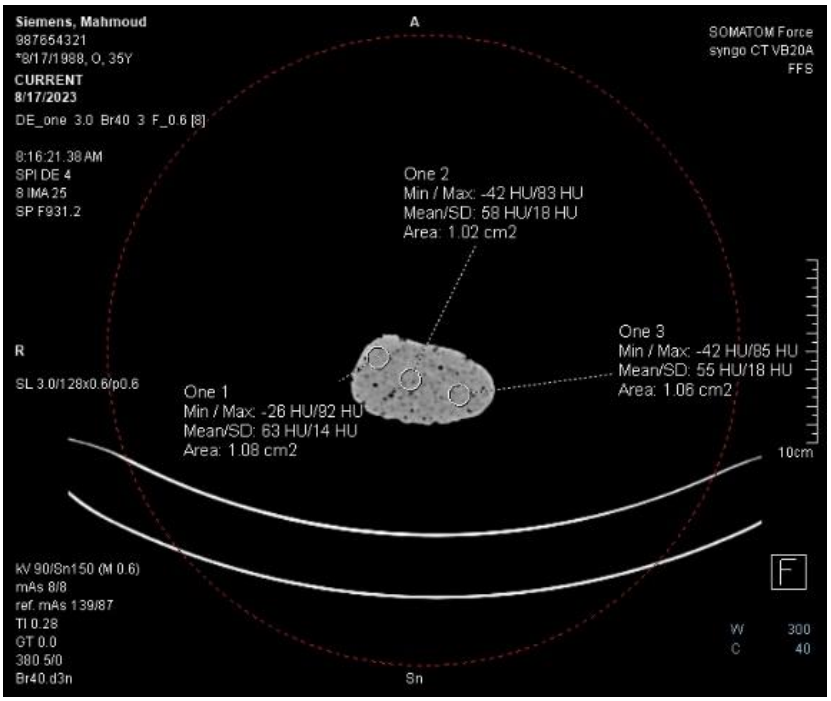

Figure 6. Sample number one analysis using MM Reading

Table 2. Sample number one HU values

Reading	min HU	max HU	Mean	SD
1	-26	92	63	18
2	-42	83	58	**14**
3	-42	85	55	18
mean value	**-36.6666667**	**86.66666667**	**58.67**	16.66666667

4.1.3 Sample Number Two

Sample number two (Figure **7**) had a min HU of 148 and max HU of 228, and the average was 194 (Table 3). The values from this sample and on will be higher due to the added iodine contrast medium.

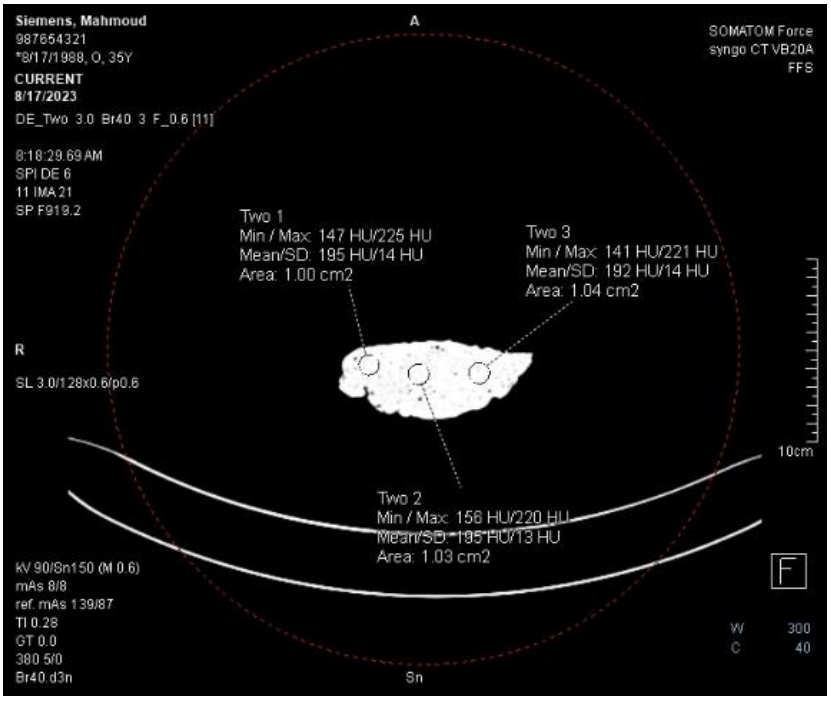

Figure 7. Sample number two analysis using MM Reading

Table 3. Sample number two HU values

Reading	min HU	max HU	Mean	SD
1	**147**	**225**	**195**	**14**
2	**156**	**220**	**195**	**13**
3	**141**	**221**	**192**	**14**
mean value	**148**	**222**	**194**	**13.66666667**

4.1.4 Sample Number Three

Sample number three (Figure 8) had the highest mass of fat (20 g), and its values were as follows; min HU was 108 and the max HU was 206, while the mean was 181 HU (Table 4).

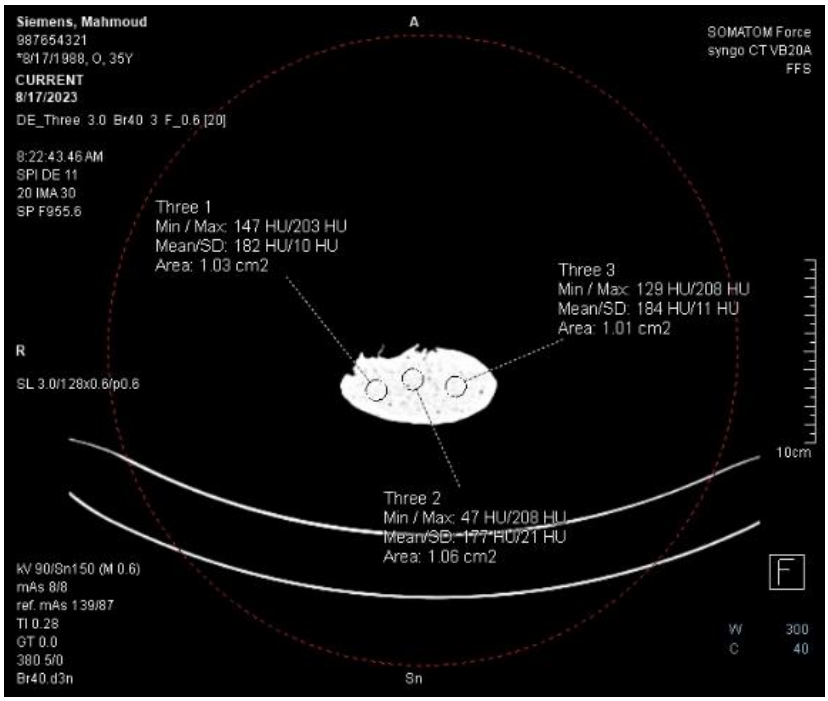

Figure 8. Sample number three analysis using MM Reading

Table 4. Sample number three HU values

Reading	min HU	max HU	Mean	SD
1	147	203	182	10
2	47	208	177	21
3	129	208	184	11
mean value	107.6666667	206.3333333	181	14

4.1.5 Sample Number Four

Sample number four (Figure 9) had a min HU of 94 and max HU of 214, whereas the mean value was 186 HU (Table 5), again, the mean value dropped in comparison to the previous (number two) sample due to the higher amount of fat added.

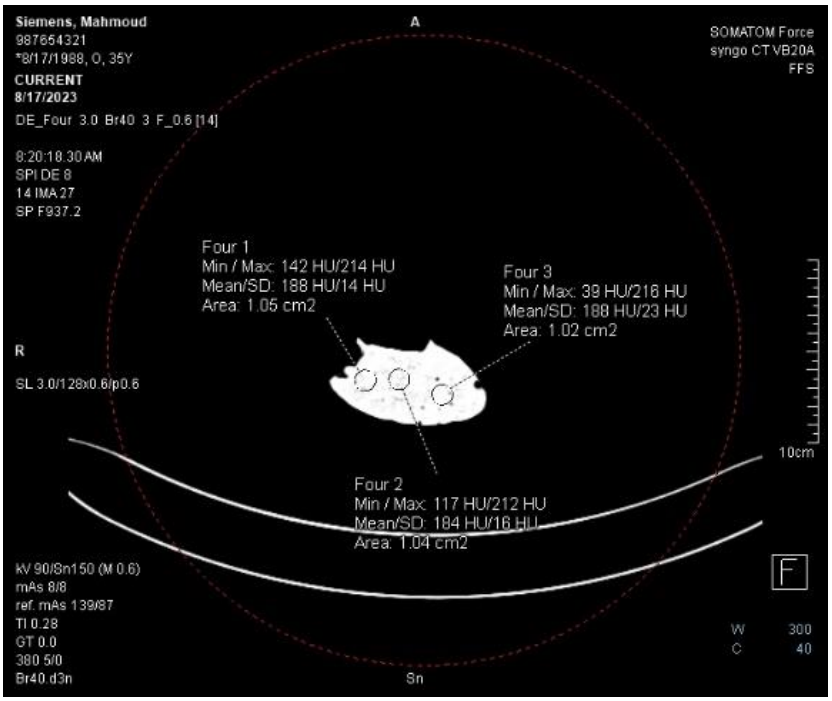

Figure 9. Sample number four analysis using MM Reading

Table 5. Sample number four HU values

Reading	min HU	max HU	Mean	SD
1	142	214	188	14
2	100	211	183	16
3	39	216	188	23
mean value	93.66666667	213.6666667	186.3	17.66666667

4.2 Dual Energy Analysis

The second analyses were done using CT Dual Energy workflow, specifically Liver VNC (virtual non contrast) application and the Fat Saturation algorithm, the special tool of measurement that is called DE Region of Interest. This time, the readings were slightly different since this application uses the special algorithm of three-material decomposition: fat, soft tissue, and contrast media.

The readings in this workflow will be as follows; VNC, CM, Mixed [(0.6) this ratio corresponds to the ratio of content between low energy dataset and high energy dataset] and Fat Fraction percentage.

The reference sample (Figure 10) and the number one sample (Figure 11) will not have appropriate readings using the Liver VNC application since both samples had no contrast medium injected, thus the algorithm lacks one material of the three-materials needed for calculations, and the reference sample had no added fat as well. Below are two images of the analyses of these two samples showing irrational results for fat saturation.

4.2.1 Reference Sample

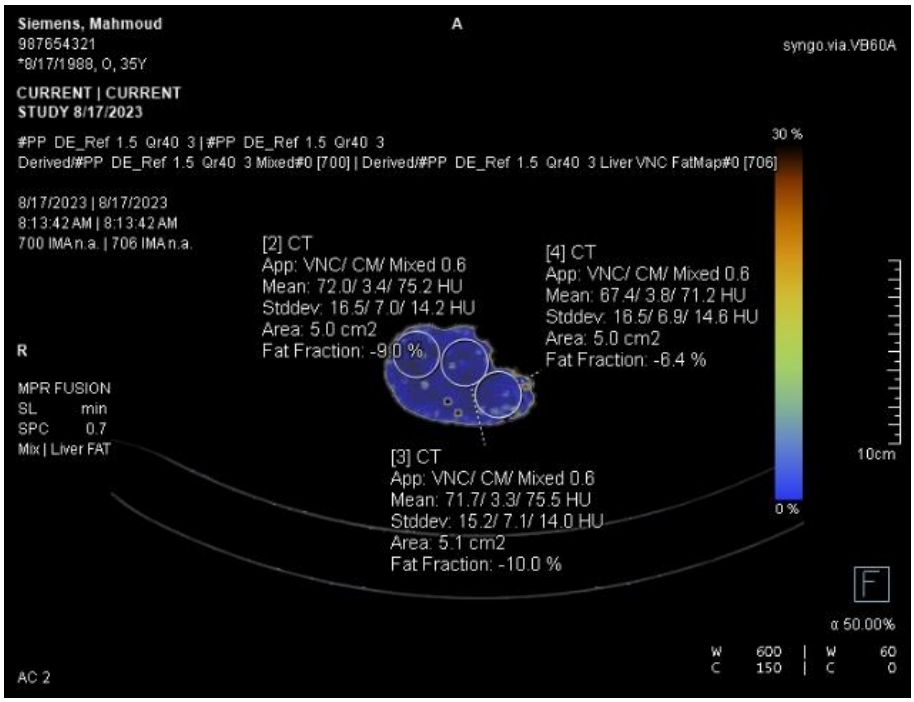

Figure 10. Reference sample analysis using CT Dual Energy workflow.

4.2.2 Sample Number One

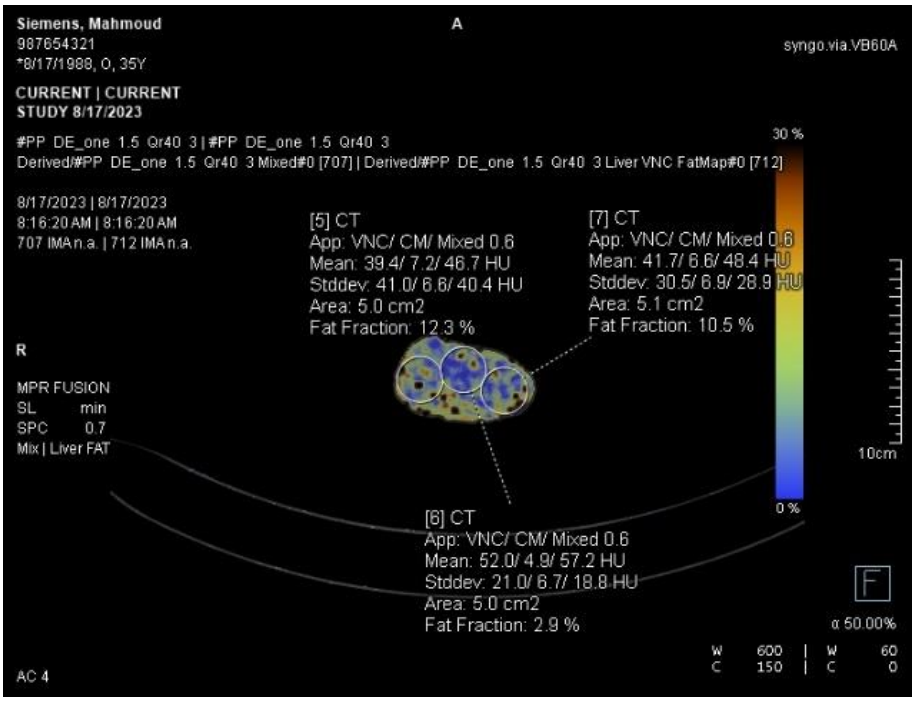

Figure 11. Sample number one analysis using CT Dual Energy workflow.

4.2.3 Sample Number Two

Sample number two (Figure 12) had a value of 57 HU for VNC, 132 HU for CM, 189 HU for mixed, and 3% Fat Fraction (Table 6). The added fat was 5g, and the total sample weight is 212g.

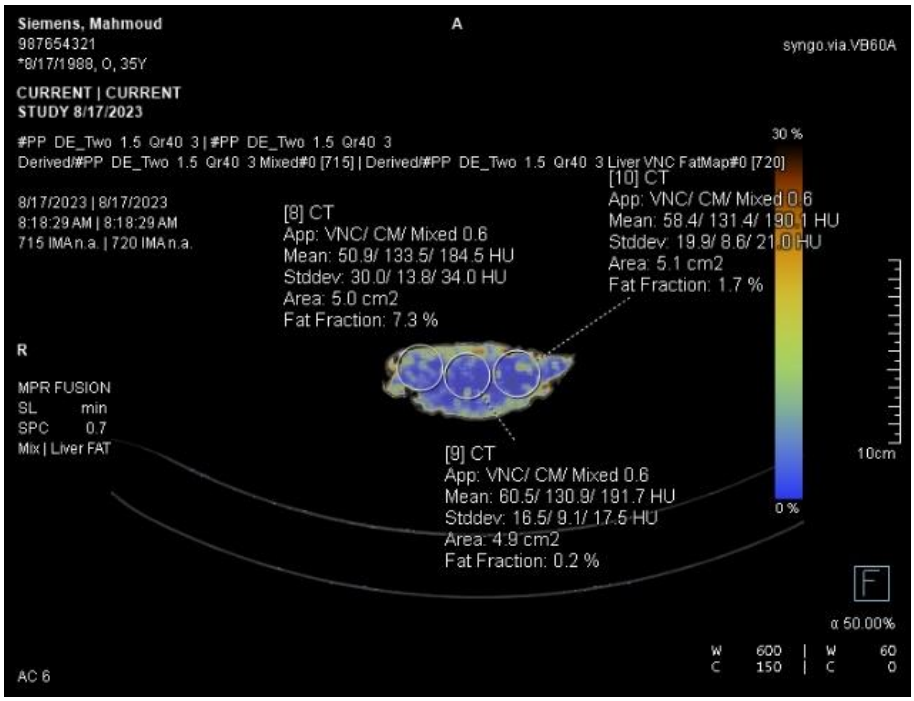

Figure 12. Sample number two analysis using CT Dual Energy workflow.

Table 6. Sample number two DE values

Reading	VNC	CM	Mixed 0.6	Fat Fraction	SD (Mixed)
1	50.9	133.5	184.5	7%	34
2	60.5	130.9	191.7	0%	17.5
3	58.4	131.4	190.1	1.70%	21
mean value	56.6	131.9333333	188.7666667	3%	24.1666667

4.2.4 Sample Number Three

Sample number three (Figure 13) had the largest amount of fat of 20g, and the total sample weight was 223g. The readings were as follows; VNC value 46 HU, CM value 131 HU, Mixed value 177 HU, and the Fat Fraction percentage was 10% (Table **7**).

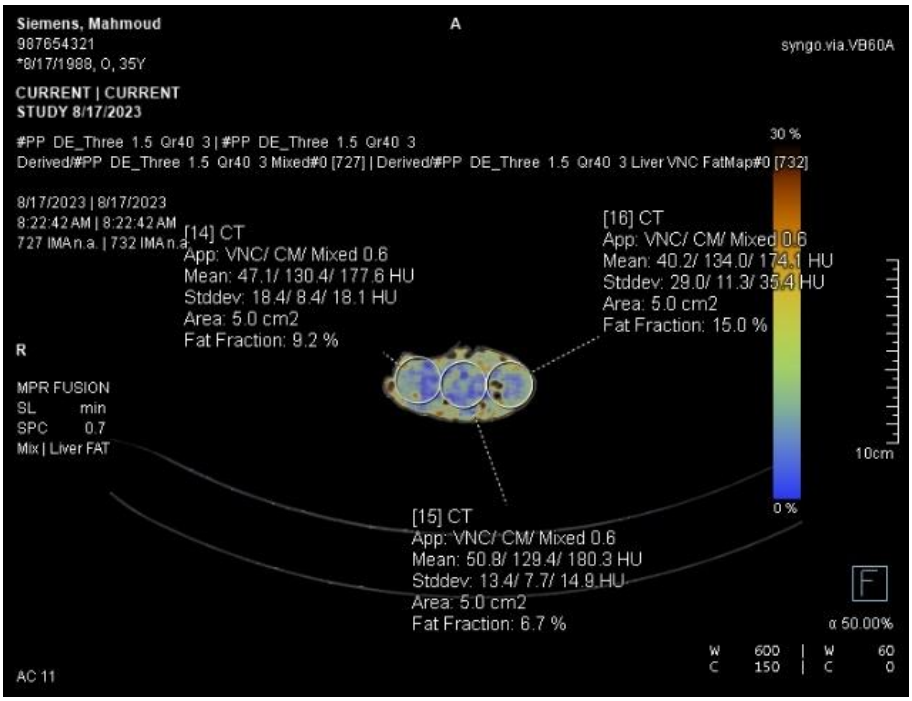

Figure 13. Sample number three analysis using CT Dual Energy workflow.

Table 7. Sample number three DE values

Reading	VNC	CM	Mixed 0.6	Fat Fraction	SD (Mixed)
1	47.1	130.4	177.6	9%	18.1
2	50.8	129.4	180.3	7%	14.9
3	40.2	134	174.1	15.00%	35.4
mean value	46.03333333	131.2666667	177.3333333	10%	22.8

4.2.5 Sample Number Four

Sample number four (Figure 14) had a 53 HU value for VNC, 130 HU for CM, 183 HU for Mixed, and 5% Fat Fraction (Table **8**). The added fat was 10g, and the total sample weight was 209g.

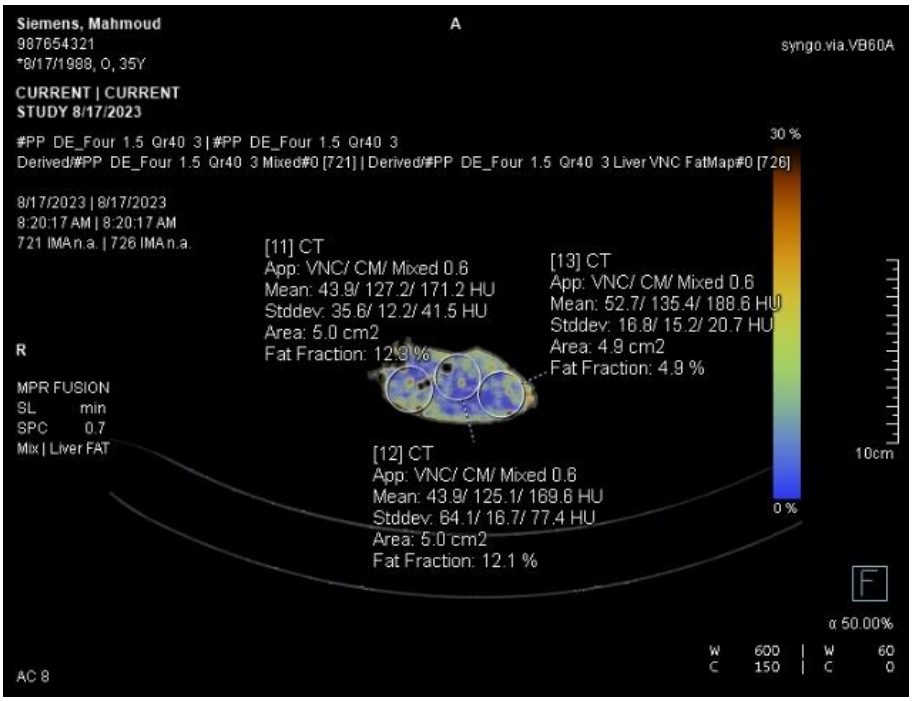

Figure 14. Sample number four analysis using CT Dual Energy workflow.

Table 8. Sample number four DE values

Reading	VNC	CM	Mixed 0.6	Fat Fraction	SD (Mixed)
1	53.3	124.3	177.9	5%	41.5
2	54.1	129.4	183.5	5%	77.4
3	52.7	135.4	188.6	4.90%	20.7
mean value	53.366667	129.7	183.3333333	5%	46.53333333

Chapter 5

Discussion

The present study demonstrates the utility of dual-source dual-energy computed tomography (DECT) for quantifying liver fat content using a controlled experimental setup with bovine liver samples supplemented with sheep fat and iodinated contrast media. The results support the hypothesis that fat fraction quantification by DECT shows a strong correlation with the manually added fat concentrations, thus furthering its potential as a non-invasive tool for the diagnosis of hepatic steatosis. This discussion places these findings in literature, discusses methodologic concerns, and addresses clinical implications.

The primary study result, a linear relationship between manually added fat and DECT-derived fat fractions, technically validates the Siemens Syngo.via Liver Virtual Non-Contrast (VNC) software. Manually adding 5 g of fat (2.4% of sample weight) yielded a 3% fat fraction, while 20 g (9% weight) yielded 10% (Figure 10–12, Tables 6–8). The results are consistent with prior DECT studies in animal models. (Kawata, 1984) also described similar attenuation reductions in rabbit livers on high-fat diets, where HU values decreased proportionally to histologically confirmed fat content. Of specific interest, the current study's use of tri-material decomposition (fat, soft tissue, iodine) transcends a basic limitation of conventional CT: the confounding effect of contrast media. Unlike single-energy CT, which struggles to differentiate between iodine-enhanced tissues and fat (Park et al., 2006), DECT takes advantage of spectral separation to differentiate fat attenuation. This is in line with (Hur et al., 2014), who demonstrated that contrast-enhanced DECT achieved similar

accuracy to non-contrast MRI for hepatic fat quantification, pointing out its clinical usefulness.

The reference sample's mean HU value (84 HU) closely matched human liver attenuation values (50–75 HU) reported by (Huo et al., 2019b) confirming that bovine liver is an excellent surrogate for human tissue in models. Reduction in HU as noted in fat-supplemented samples (e.g., Sample 1: 59 HU compared to Reference: 84 HU) is suggestive of fat's inherent negative attenuation (−50 to −100 HU)(Chougule et al., 2018). This inverse correlation between fat density and HU has been amply demonstrated in animal (Kodama et al., 2007) and human studies (Zeb et al., 2012). But the study sophisticates the paradigm by demonstrating that DECT can achieve this even under contrast-enhanced conditions, which the conventional CT cannot (Park et al., 2006).

Non-alcoholic fatty liver disease (NAFLD) is a common liver disease in Mediterranean countries, often linked with diets rich in carbohydrates and saturated fats. Early detection of hepatic steatosis is vital to prevent its progression to more serious entities, such as nonalcoholic steatohepatitis (NASH) or cirrhosis. While liver biopsy is the gold standard diagnostic available, its invasive nature and potential for sampling heterogeneity render it unsuitable for dynamic monitoring of chronic disease. Magnetic resonance imaging proton density fat fraction (PDFF) is an extremely sensitive tool to detect liver fat but, as an expensive analytical method, limits its widespread use, particularly in low-resource areas. The recent development of dual-energy computed tomography (DECT) is a faster and more cost-effective alternative. The results align with (Xu et al., 2022), which reported a strong correlation ($r = 0.89$, $p < 0.001$) between fat fractions from contrast-enhanced DECT and MRI-PDFF in human patients. This indicates that DECT may aid in overcoming diagnostic difficulties in areas with limited MRI availability.

Additionally, the experimental design of the study, utilizing iodinated contrast to simulate clinical conditions, highlights the particular strength of DECT in post-contrast fat quantitation. Single-energy CT is faced with difficulty in this aspect due to the overlapping attenuation values of iodine and parenchymal tissues (Park et al., 2006). DECT, however, with its material decomposition algorithm, distinguishes iodine (high Z-number) from fat, enabling precise calculation of the fat fraction regardless of contrast enhancement. This skill is most critical in patients undergoing multiphasic imaging of the liver, where incidental steatosis detection can impact treatment without additional imaging.

Chapter 6

Conclusions and Recommendations

6.1 Conclusions

The fat fraction percentage, and the high level of fat within the liver which leads to hepatic steatosis (the histologic term), are all very crucial factors to check and be aware of; especially in our Mediterranean region as we rely on a diet that promotes the accumulation of fat in the liver, which leads to non-alcoholic fatty liver disease. Another very important case to study the fat content of the liver is to check the possibility of liver donation as this procedure is one of the most wanted globally. The use of dual source dual energy CT has shown promising results of fat fraction in the study, which can provide evidence to be used clinically by the relevant clinicians. A larger number of samples would enhance the reliability of the results, but the drawback would be the use of more than one animal liver to conduct the study (one liver weighs about 1 kg). DECT's added diagnostic value provides important information to spare the patient unnecessary invasive procedures where possible unless further assessment is needed.

6.2 Limitations and Challenges

The main limitation to this study was the lack of needed instruments (SOMATOM Force scanner) in the state of Palestine, which obliged me to scan the samples in (Wolfson Medical Center). The air bubbles in the mixture caused the high noise readings in the regions of interests. The small sample size (n = 5), although each sample scanned multiple times, limits statistical power of the study.

6.3 Recommendations

1. Further studies on the role of DECT should be made in the state of Palestine.
2. Vacuum sealing may be employed in future protocols to minimize air entrapment.
3. Larger number of samples would enhance the results, multiple cows' livers can be mixed in the mincing process.
4. Performing the model of this study in correlation with other modalities, especially with MRI.

References

Ambrose, J. (1996). You Never Know What is Just around the Next Corner. *Rivista Di Neuroradiologia*, *9*(4), 399–404. https://doi.org/10.1177/197140099600900407

Ashtari, S. (2015). Non-alcohol fatty liver disease in Asia: Prevention and planning. *World Journal of Hepatology*, *7*(13), 1788. https://doi.org/10.4254/wjh.v7.i13.1788

Boyce, C. J., Pickhardt, P. J., Kim, D. H., Taylor, A. J., Winter, T. C., Bruce, R. J., Lindstrom, M. J., & Hinshaw, J. L. (2010). Hepatic Steatosis (Fatty Liver Disease) in Asymptomatic Adults Identified by Unenhanced Low-Dose CT. *American Journal of Roentgenology*, *194*(3), 623–628. https://doi.org/10.2214/AJR.09.2590

Clinical Case Study Spine Modeling for Minimum Invasive Spine Surgeries Using Rapid Prototyping (February 2018).

Diehl, A. M., & Day, C. (2017). Cause, Pathogenesis, and Treatment of Nonalcoholic Steatohepatitis. *New England Journal of Medicine*, *377*(21), 2063–2072. https://doi.org/10.1056/nejmra1503519

Estermann, S.-J., Förster-Streffleur, S., Hirtler, L., Streicher, J., Pahr, D. H., & Reisinger, A. (2021). Comparison of Thiel preserved, fresh human, and animal liver tissue in terms of mechanical properties. *Annals of Anatomy - Anatomischer Anzeiger*, *236*, 151717. https://doi.org/10.1016/j.aanat.2021.151717

Euclid Seeram. (2015). *Computed Tomography Physical Principles, Clinical Application* (4th ed., Vol. 4). Elsevier.

Fleischmann, D., & Boas, F. E. (2011). Computed tomography—old ideas and new technology. *European Radiology*, *21*(3), 510–517. https://doi.org/10.1007/s00330-011-2056-z

Friedman, S. L., Neuschwander-Tetri, B. A., Rinella, M., & Sanyal, A. J. (2018). Mechanisms of NAFLD development and therapeutic strategies. In *Nature Medicine* (Vol. 24, Issue 7, pp. 908–922). Nature Publishing Group. https://doi.org/10.1038/s41591-018-0104-9

Gao, B., & Bataller, R. (2011). Alcoholic liver disease: Pathogenesis and new therapeutic targets. *Gastroenterology*, *141*(5), 1572–1585. https://doi.org/10.1053/j.gastro.2011.09.002

Hao, F., Cubero, F. J., Ramadori, P., Liao, L., Haas, U., Lambertz, D., Sonntag, R., Bangen, J. M., Gassler, N., Hoss, M., Streetz, K. L., Reissing, J., Zimmermann, H. W., Trautwein, C., Liedtke, C., & Nevzorova, Y. A. (2017). Inhibition of Caspase-8 does not protect from alcohol-induced liver apoptosis but alleviates alcoholic hepatic steatosis in mice. *Cell Death and Disease*, *8*(10). https://doi.org/10.1038/CDDIS.2017.532

Hayre, C. M., & Chau, S. (2022). *Computed Tomography: A Primer for Radiographers* (1st ed.), 3-44. CRC Press. https://doi.org/10.1201/9781003132554

Hounsfield, G. N. (1973). Computerized transverse axial scanning (tomography): Part 1. Description of system. *The British Journal of Radiology*, *46*(552), 1016–1022. https://doi.org/10.1259/0007-1285-46-552-1016

Huo, Y., Terry, J. G., Wang, J., Nair, S., Lasko, T. A., Freedman, B. I., Carr, J. J., & Landman, B. A. (2019). Fully automatic liver attenuation estimation combing CNN segmentation and morphological operations. *Medical Physics*, *46*(8), 3508–3519. https://doi.org/10.1002/mp.13675

Hur, B. Y., Lee, J. M., Hyunsik, W., Lee, K. B., Joo, I., Han, J. K., & Choi, B. I. (2014). Quantification of the Fat Fraction in the Liver Using Dual-Energy Computed Tomography and Multimaterial Decomposition. *Journal of Computer Assisted Tomography*, *38*(6), 845–852. https://doi.org/10.1097/RCT.0000000000000142

Johnson, T. R. C., Krauß, B., Sedlmair, M., Grasruck, M., Bruder, H., Morhard, D., Fink, C., Weckbach, S., Lenhard, M., Schmidt, B., Flohr, T., Reiser, M. F., & Becker, C. R. (2007). Material differentiation by dual energy CT: initial experience. *European Radiology*, *17*(6), 1510–1517. https://doi.org/10.1007/s00330-006-0517-6

Kauczor, H., Parizel, P. M., G Peh Konstantinn Nikolaouu, W. C., Andreaa Laghii, F., & Rubin Editors, G. (2019). *Medical Radiology · Diagnostic Imaging Series Editors: Multislice CT Fourth Edition* (4th ed.). http://www.springer.com/series/4354

Kauczor, H.-U., Parizel, P. M., Peh, W. C. G., Andréééuler, H., & Dushyanttsahaniieditors, D. (2022). *Medical Radiology· Diagnostic Imaging Series Editors: Spectral Imaging Dual-Energy, Multi-Energy and Photon-Counting CT*. https://doi.org/https://doi.org/10.1007/978-3-030-96285-2

Kawata, R., Sakata, K., Kunieda, T., Saji, S., Doi, H., & Nozawa, Y. (1984). Quantitative evaluation of fatty liver by computed tomography in rabbits. *American Journal of Roentgenology*, *142*(4), 741–746. https://doi.org/10.2214/ajr.142.4.741

Kodama, Y., Ng, C. S., Wu, T. T., Ayers, G. D., Curley, S. A., Abdalla, E. K., Vauthey, J. N., & Charnsangavej, C. (2007). Comparison of CT Methods for Determining the Fat Content of the Liver. *American Journal of Roentgenology*, *188*(5), 1307–1312. https://doi.org/10.2214/AJR.06.0992

Kriston, A., Mendonça, P., Silva, A., Paden, R. G., Pavlicek, W., Sahani, D., Janos Kis, B., Rusko, L., Okerlund, D., & Bhotika, R. (2011). Liver fat quantification using fast kVp-switching dual energy CT. In B. M. Dawant & D. R. Haynor (Eds.), *Medical Imaging 2011: Image Processing* (Vol. 7962, p. 1-8). SPIE. https://doi.org/10.1117/12.878206

Mahesh, M. (2013). The Essential Physics of Medical Imaging, Third Edition. *Medical Physics*, *40*(7). https://doi.org/10.1118/1.4811156

Mamourian Alexander C. (2013). *CT Imaging practical physics, artifacts and pitfalls* (1st ed., Vol. 1 pp: 2-33). Oxford University Press.

Mirmiran, P., Amirhamidi, Z., Ejtahed, H.-S., Bahadoran, Z., & Azizi, F. (2017). Relationship between Diet and Non-alcoholic Fatty Liver Disease: A Review Article. *Iranian Journal of Public Health*, *46*(8), 1007–1017. http://www.ncbi.nlm.nih.gov/pubmed/28894701

Park, S. H., Kim, P. N., Kim, K. W., Lee, S. W., Yoon, S. E., Park, S. W., Ha, H. K., Lee, M. G., Hwang, S., Lee, S. G., Yu, E. S., & Cho, E. Y. (2006). Macrovesicular hepatic steatosis in living liver donors: Use of CT for quantitative and qualitative assessment. In *Radiology* (Vol. 239, Issue 1, pp. 105–112). https://doi.org/10.1148/radiol.2391050361

Romans Lois E. (2018). *Computed Tomography for Technologists: A Comprehensive Text* (Pete Sabatini, Ed.; 2nd ed.). Lippincott Williams & Wilkins.

Su, Z. Z., Shan, H., He, B. J., Lv, W. T., Meng, X. C., Wang, J., Zhu, K. S., Yang, Y., & Chen, G. H. (2009). Selection of the most powerful predictors for the evaluation of hepatic steatosis grade: An experimental study. *European Journal of Radiology*, *72*(1), 118–124. https://doi.org/10.1016/j.ejrad.2008.06.020

Xu, J. J., Boesen, M. R., Hansen, S. L., Ulriksen, P. S., Holm, S., Lönn, L., & Hansen, K. L. (2022). Assessment of Liver Fat: Dual-Energy CT versus Conventional CT with and without Contrast. *Diagnostics*, *12*(3), 708. https://doi.org/10.3390/diagnostics12030708

Younossi, Z. M., Koenig, A. B., Abdelatif, D., Fazel, Y., Henry, L., & Wymer, M. (2016). Global epidemiology of nonalcoholic fatty liver disease—Meta-analytic assessment of prevalence, incidence, and outcomes. *Hepatology*, *64*(1), 73–84. https://doi.org/10.1002/hep.28431

Zeb, I., Li, D., Nasir, K., Katz, R., Larijani, V. N., & Budoff, M. J. (2012). Computed Tomography Scans in the Evaluation of Fatty Liver Disease in a Population Based Study. *Academic Radiology*, *19*(7), 811–818. https://doi.org/10.1016/j.acra.2012.02.022

قياس تركيز الدهون في الكبد باستخدام التصوير الطبقي المحوسب ثنائي المصدر مزدوج الطاقة الإشعاعية.

إعداد: محمود ماهر فاخوري

إشراف: د. محمد الحجوج

الملخص

تم الشروع في هذه الدراسة القائمة على حساب نسبة الدهون المتراكمة في الكبد بسبب النسبة الكبيرة من سكان حوض البحر المتوسط المصابين بالتليف الكبدي الغير كحولي، وذلك يرجع إلى النظام الغذائي المتبع في هذه الدول والمعتمد بشكل كبير على المخبوزات والخمائر، بالإضافة إلى الوزن الزائد والسمنة.

تم استخدام كبد حيواني (عجل) وتم طحنه وذلك للحصول على التجانس المطلوب عند اضافة المواد فيما بعد، وتم تقسيم هذا الكبد بعد الطحن إلى خمس عينات متقاربة في الوزن.

العينة الاولى تم اعتبارها عينة مرجعية ولم يضف لها اي مواد. باقي العينات تم اضافة مادة أو مادتين للعينة بعد الطحن. المواد المضافة هي عبارة عن مادة ملونّة تستخدم في التصوير الطبي وتحتوي على اليود وتم اضافتها لثلاث عينات، وكذلك تم استخدام دهن خروف مذاب وتم اضافته لأربعة من العينات.

تم تصوير العينات باستخدام جهاز التصوير الطبقي ثنائي الأنبوبات وثنائي الطاقات الإشعاعية من شركة سيمنز العالمية، وباستخدام البروتوكول المتبع في المستشفيات لتصوير الكبد. الصور الناتجة من هذا التصوير تم تحليلها بواسطة البرنامج الخاص بشركة سيمنز العالمية بنسخته الأخيرة المتوفرة في سوق العمل.

أظهرت النتائج وجود علاقة قوية بين كمية الدهون المضافة فعليًا إلى العينات ونسب الدهون المحسوبة بواسطة التصوير الطبقي ثنائي الطاقة. على سبيل المثال، عند إضافة 5 جرام من الدهون (2.4% من وزن العينة الكلي)، تم الحصول

على نسبة دهون قدرها 3%، بينما عند إضافة 20 جرام من الدهون (9% من وزن العينة الكلي)، تم الحصول على نسبة دهون قدرها 10%. أكدت الدراسة إمكانية الاعتماد على التصوير الطبقي ثنائي الطاقة في قياس نسبة الدهون في الكبد بدقة عالية.

هذا البحث يعد خطوة في الاتجاه للتقليل من الاعباء والأوجاع التي يتعرض لها المريض عند خضوعه لفحص خزعة مخبرية للكبد لفحص نسبة الدهون، وكما أنه يعد أرخص تكلفة من فحص التصوير المغناطيسي.